

PAPER • OPEN ACCESS

Optical and Coupled-Channels Description of $^{20}\text{Ne} + ^{16}\text{O}$ Elastic Scattering

To cite this article: N Burtebayev *et al* 2015 *J. Phys.: Conf. Ser.* **590** 012056

View the [article online](#) for updates and enhancements.

You may also like

- [Nucleon scattering analysis with a lane-consistent dispersive optical potential for Hf, W and Ta isotopes](#)

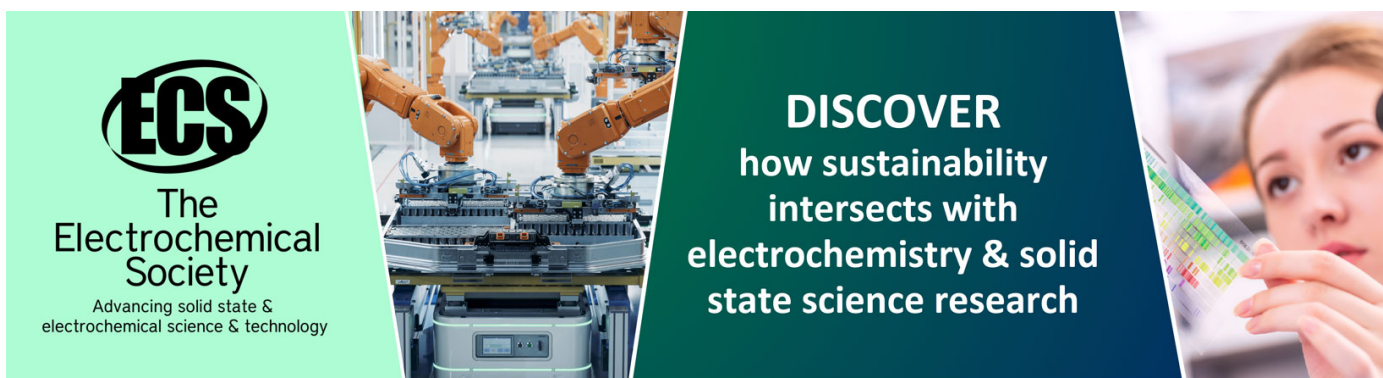
Xiuniao Zhao, Weili Sun, E Sh Soukhovitski *et al.*

- [Analysis of neutron bound states of \$^{208}\text{Pb}\$ by a dispersive optical model potential](#)

Xiuniao Zhao, Weili Sun, E Sh Soukhovitski *et al.*

- [Multi-hump potentials for efficient wave absorption in the numerical solution of the time-dependent Schrödinger equation](#)

A A Silaev, A A Romanov and N V Vvedenskii



ECS
The
Electrochemical
Society
Advancing solid state &
electrochemical science & technology

DISCOVER
how sustainability
intersects with
electrochemistry & solid
state science research

Optical and Coupled-Channels Description of $^{20}\text{Ne}+^{16}\text{O}$ Elastic Scattering

N Burtebayev¹, M Nassurlla^{1,4}, D Alimov^{1,4}, I Boztosun^{2,3},
J Burtebayeva¹, A K Morzabayev⁵, S K Sakhiev⁵, S V Artemov⁶,
J M Mussaev⁷

¹ Institute of Nuclear Physics, 050032, Almaty, Kazakhstan,

² Akdeniz University, Faculty of Science, Department of Physics, 07058, Antalya, Turkey,

³ Akdeniz University, Nuclear Sciences Application and Research Center - NUBA, 07058 Antalya, Turkey,

⁴ Kazakh National University, Almaty, Kazakhstan,

⁵ Eurasia National University, Astana, Kazakhstan,

⁶ Institute of Nuclear Physics, Tashkent, Uzbekistan,

⁷ South Kazakhstan State University, Shymkent, Kazakhstan.

E-mail: boztosun@akdeniz.edu.tr

Abstract. The elastic scattering of the $^{20}\text{Ne}+^{16}\text{O}$ system has been analyzed with a phenomenological potential approach within the framework of the optical and coupled-channels models at $E_{Lab}=50.0$ MeV. The striking feature of the experimental data is the oscillatory structure at the intermediate angles and a rapid increase at large angles. Optical potentials have difficulty in describing such structures and predict a fall of experimental data around the intermediate angles. In order to explain this structure, we have used a deep real potential with a sum of Woods-Saxon typed surface and volume imaginary potentials. We present that deep real potential with these imaginary potentials explain the oscillatory structure and backward rise observed in the elastic scattering data within both models. It should be pointed out that there is a magnitude problem of the inelastic 2^+ data for the deformed ^{20}Ne nucleus that the standard coupled-channels model is unable to predict correctly.

1. Introduction

The elastic and inelastic scattering of $4N$ -type nuclei have taken a great deal of interest and have been amongst the main sources of information about the structure of complex nuclei over the years [1, 2, 3, 4, 5, 6, 7]. There have been numerous experimental and theoretical investigations to understand the structure and reactions of sp -shell and $4N$ -type α -structured nuclei, and these investigations for the nuclear reactions have displayed a common unexpected feature near $\theta_{CM}=180^\circ$ for the elastic and inelastic scattering cross-sections. The scattering of α -particles and strongly clusterized heavy ions from light nuclei is an example that one can observe a significant cross section enhancement at backward angles, which in some cases is due to exchange of α -particles between the interacting nuclei [8, 9, 10, 11, 12, 13].

The experimental data for the $^{20}\text{Ne}+^{16}\text{O}$ system has been measured by Stock *et al.* [14] and it exhibits an oscillatory structure at the intermediate angles and a rapid increase at large angles. Optical potentials proposed to explain the experimental data have failed to describe the oscillatory structure at intermediate angles and also the backward rise within the framework of



the optical model. In a recent study, Yang and Li [15] have investigated the $^{20}\text{Ne}+^{16}\text{O}$ system in the energy range of $E_{c.m.} = 24.5$ to 35.5 MeV by using a folding potential based on the four- α -particle model for the ^{16}O nucleus and the $\alpha+^{16}\text{O}$ model for the ^{20}Ne nucleus. They have obtained a reasonable description of the experimental data for these energies. However, the physical origin of the observed structure is not yet fully understood [16] and interpreted as an exchange of α -particle between projectile and target nuclei as Yang and Li [15] underlined.

In this paper, as a part of our further experimental and theoretical research in the future, we first attempt to explain the elastic scattering data of $^{20}\text{Ne}+^{16}\text{O}$ system at 50 MeV by using a deep real and imaginary potentials within the framework of optical model. It is known that the inclusion of the excited states of the target nucleus in the coupled-channels calculations may have a significant effect on the scattering. Therefore, we have also conducted coupled-channels calculations to observe this effect.

In the next section, we introduce our Optical model and potential parameters to explain the observed experimental data. Then, we show the results of optical and coupled-channels model analyzes in Section 3. Our conclusion is given in Section 4.

2. The Model

The standard Optical model with folding model potentials or with similar phenomenological potentials such as the square of the Woods-Saxon has failed to describe certain aspects of the experimental data, particularly the oscillatory structure observed in the experimental data and the description of the inelastic scattering data. Therefore, in the present calculations, we use a deep real potential with a volume and surface type imaginary potentials [17]. Our total real potential consists of the nuclear potential, $V_{Nuclear}$, and the Coulomb and centrifugal potentials, V_{Coul} , V_{Cent} respectively

$$V_{total}(r) = V_{Nuclear}(r) + V_{Coulomb}(r) + V_{Centrifugal}(r) \quad (1)$$

The nuclear potential is assumed to have the square of a Woods-Saxon shape:

$$V_{Nuclear}(r) = \frac{-V_0}{(1 + \exp(r - R)/a)^2} \quad (2)$$

where $V_0=740.0$ MeV and $R=r_0(A_a^{1/3}+A_A^{1/3})$ with $r_0=0.680$ fm and $a=1.36$ fm.

The Coulomb potential [17] due to a charge $Z_a e$ interacting with a charge $Z_A e$, distributed uniformly over a sphere of radius R_c , is also added.

$$V_{Coulomb}(r) = \frac{1}{4\pi\epsilon_0} \frac{Z_a Z_A e^2}{r}, \quad r \geq R_c \quad (3)$$

$$= \frac{1}{4\pi\epsilon_0} \frac{Z_a Z_A e^2}{2R_c} \left(3 - \frac{r^2}{R_c^2}\right), \quad r < R_c \quad (4)$$

where $R_c=5.76$ fm is the Coulomb radius, and Z_a and Z_A denote the charges of the projectile a and the target nuclei A respectively.

The sum of the nuclear, Coulomb and the centrifugal potentials is shown in Fig. 1 for various values of the orbital angular momentum. The superposition of the attractive and repulsive potentials results in the formation of a potential pocket. The width and depth of the pocket depend on the orbital angular momentum quantum number for a given nuclear potential. This pocket is very important for the interference of the barrier and internal waves, which creates the oscillatory structure observed in the cross-section [17].

The imaginary part of the potential was taken as the sum of a Woods-Saxon volume and the surface potentials:

$$W(r) = -W_V f(r, R_V, a_V) + 4W_S a_S df(r, R_S, a_S)/dr \quad (5)$$

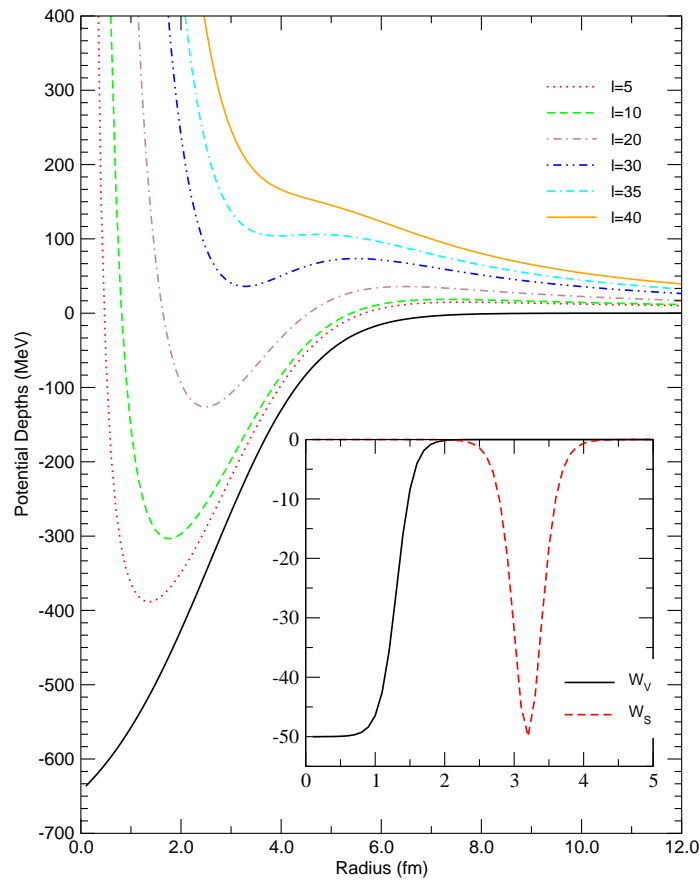


Figure 1. Interaction potential between ^{16}O and ^{20}Ne for various values of the orbital angular momentum quantum number, l . The parameters are given in the text.

$$f(r, R, a) = \frac{1}{(1 + \exp((r - R)/a))} \quad (6)$$

with $W_V=50.0$ MeV, $r_V=0.250$, $a_V=0.120$ fm and $W_S=50.0$ MeV, $r_S=0.610$, $a_S=0.140$ fm.

The shape of the imaginary potentials are shown in the inset of Fig. 1 for $E_{Lab}=50.0$ MeV. The relative significance of the volume and surface components of the imaginary potential is also studied for this energy. Removing the volume component mainly changes the amplitude of the cross-section at large angles while removing the surface component increases the cross-sections at large angles. The effect of the deep real and imaginary potentials can be understood in terms of the interference between the internal and barrier waves that correspond to a decomposition [17] of the scattering amplitude into two components, the inner and external waves. The inner wave comes from the reflection at the inner face of the total real potential pocket and the external wave comes from the reflection at the outer barrier as the potential pocket is shown in Fig. 1 for the total real potential.

3. The Results

Using the above-described Optical model, we have analyzed the elastic scattering data of the $^{20}\text{Ne}+^{16}\text{O}$ system at 50.0 MeV in the laboratory system. The comparisons between experimental data and the Optical model fits are shown in Fig. 2. In this figure, we have also presented the prediction of the optical potential of Ref. [14]. As it can be seen from this figure, the optical

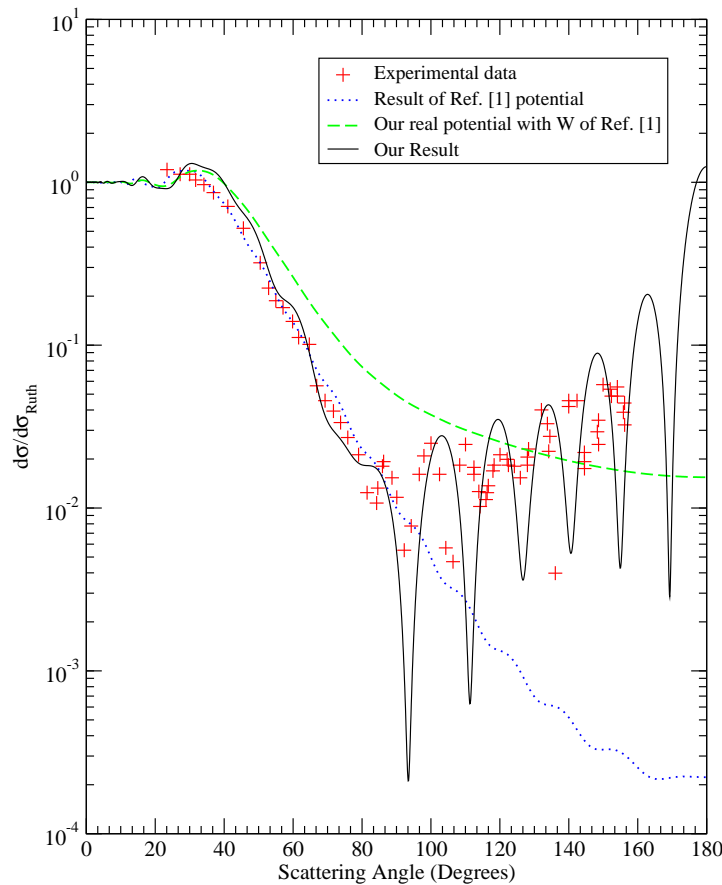


Figure 2. The effect of the two imaginary potentials: Dotted line is the prediction of the potential of Ref. [14] while dashed line is the result of our deep real potential with the imaginary potential of Ref. [14]. Solid line is our prediction with deep real potential with the sum of volume and surface imaginary potentials.

potential describes the experimental data at the forward angles up to 90° and then theoretical prediction falls off and unable to reproduce the oscillatory structure and rises at large angles. Therefore, we have used a deep real potential with the imaginary potential of Ref. [14] and it increases the magnitude of the cross-section but it is still unable to produce the oscillatory structure observed in the experimental data. By using the above-described imaginary potentials given in the Model section, we have obtained a reasonable agreement with the experimental data over all angles measured. A good agreement between the experimental data and our prediction is obtained at the forward angles and the oscillatory structure is reproduced at intermediate and backward angles.

In order to see the coupling effect on the scattering observables, we have conducted coupled-channels calculations by deforming the projectile ^{20}Ne to treat its collective excitation explicitly in the framework of the coupled-channels formalism. It has been assumed that the projectile ^{20}Ne nucleus has a static quadrupole deformation, and that its rotation can be described in the framework of the collective rotational model. It is therefore taken into account by deforming the real optical potential in the following way

$$R(\theta, \phi) = r_0 {}^{16}\text{O}^{1/3} + r_0 {}^{20}\text{Ne}^{1/3} [1 + \beta_2 Y_{20}(\theta, \phi)] \quad (7)$$

where $\beta_2 = -0.23$ is the deformation parameter of ^{20}Ne [18]. This value should be increased in order to fit the magnitude for the 2^+ data. We have included the first excited state, 2^+ (1.78 MeV), of the projectile nucleus ^{20}Ne .

The inclusion of the 2^+ excited state has an effect on the elastic scattering fits at intermediate and large angles. However, this effect is not substantial and can be altered by changing the parameters of optical potential. Furthermore, the prediction for the 2^+ state inelastic data has a large magnitude problem. In order to get the magnitude right, we have to increase the deformation parameter enormously. We could not solve this problem but it should be studied in detail by using the α -cluster structure of ^{20}Ne and ^{16}O as well as by the inclusion of the α -transfer in the reaction calculations. This has been a long standing problem that a solution has been proposed by using a second derivative type of coupling potential [1] which should be applied to this reaction.

4. Summary

We have shown in this paper that the interaction of α -cluster structure type nuclei such as $^{20}\text{Ne}+^{16}\text{O}$ system are very sensitive to the shape of the real and imaginary potentials in the surface region. In this paper, we have first shown that the real potential, responsible to describe the scattering observables, should be deep enough to provide a pocket in the total potential for the interference of the external waves, coming from the reflection at the outer barrier and internal waves, coming from the reflection at the inner face of the total real potential pocket. Secondly, the imaginary potential should have two components located inside the real potential as a sum of volume and surface types. Volume one is responsible to account for the flux going to the inelastic channels as excitation while the surface one is responsible to take into account α -type cluster exchange occurring at the surface of interaction. Coupled-channels calculations show an effect on the elastic scattering observables but within the standard coupled-channels calculations by using the experimental deformation parameters, it is difficult to describe the excited state data. In particular, the magnitude of the inelastic data is underestimated by a large factor and without increasing the deformation parameter, the experimental data for the inelastic scattering cannot be described.

Acknowledgments

This work is partly supported by the scientific and technological research council of Turkey (TÜBİTAK) with grant number: 114F220.

- [1] Boztosun I and Rae WDM 2001 *Phys. Lett.* **518B** 229
- [2] Bremner C *et al.* 2002 *Phys. Rev. C* **66** 034605
- [3] Freer M *et al.* 2004 *Phys. Rev. C* **70** 064311
- [4] Karakoc M and Boztosun I 2006 *Phys. Rev. C* **73** 047601; 2006 *Int. J. of Mod. Phys. E* **15** 1317
- [5] Freer M *et al.* 2005 *Phys. Rev. C* **71** 047305
- [6] Kucuk Y and Boztosun I 2006 *Nucl. Phys. A* **764** 160
- [7] Freer M *et al.* 2007 *Phys. Rev. C* **76** 034320
- [8] Burtebaev N *et al.* 2005 *Phys. of Atom. Nucl.* **68** 1303
- [9] Burtebayev N *et al.* 2010 *Phys. of Atom. Nucl.* **73** 746
- [10] Burtebayev N *et al.* 2013 *Nucl. Phys. A* **909** 1303
- [11] Hamada Sh, Burtebayev N and Amangeldi N 2014 *Int. J. of Mod. Phys. E* **23** 145061
- [12] Hamada Sh, Burtebayev N, Gridnev KA and Amangeldi N 2011 *Nucl. Phys. A* **859** 29
- [13] Amar A *et al.* 2011 *Int. J. of Mod. Phys. E-Nucl. Phys.* **20** 980
- [14] Stock R *et al.* 1976 *Phys. Rev. C* **14** 1824
- [15] Yang Yong-Xu and Li Qing-Run 2011 *Phys. Rev. C* **84** 014602
- [16] Boztosun I and Rae WDM 2001 *Phys. Rev. C* **63** 054607; 2001 *Phys. Rev. C* **64** 054607; 2002 *Phys. Rev. C* **65** 024603
- [17] Boztosun I 2002 *Phys. Rev. C* **66** 024610
- [18] Stone N J 2014 *IAEA Nuclear Data Section INDC(NDS)-0658*